Computational Mechanics 19 (1997) 228 – 239 © Springer-Verlag 1997

Formulation and implementation of three-dimensional viscoelasticity at small and finite strains

M. Kaliske, H. Rothert

Abstract Purely elastic material models have a limited validity. Generally, a certain amount of energy absorbing behaviour can be observed experimentally for nearly any material. A large class of dissipative materials is described by a time- and frequency-dependent viscoelastic constitutive model. Typical representatives of this type are polymeric rubber materials. A linear viscoelastic approach at small and large strains is described in detail and this makes a very efficient numerical formulation possible. The underlying constitutive structure is the generalized Maxwell-element. The derivation of the numerical model is given. It will be shown that the developed isotropic algorithmic material tensor is even valid for the current configuration in the case of large strains. Aspects of evaluating experimental investigations as well as parameter identification are considered. Finally, finite element simulations of time-dependent deformations of rubber structures using mixed elements are presented.

1 Introduction

Besides a static structural response, the load-carrying behaviour for dynamic loading is of interest for a large number of structures and classes of materials. In this article, time- or frequency-dependent materials are considered and structures are loaded in such a way that inertial effects cannot be neglected. Typical representatives of the class of problems mentioned are polymeric structures made out of any kind of synthetic material. Generally, the large strain case with respect to polymers applies to rubber material. An interesting problem is e.g. the analysis of tires where time- and frequency-dependent stiffness and dissipative properties are of great importance. Furthermore, damping devices and coatings to reduce vibration capabilities are employed in a large number of mechanical and civil engineering structures.

Communicated by S. N. Atluri, 5 September 1996

M. Kaliske, H. Rothert
Institut für Statik, Universität Hannover, Appelstraße 9a,
30167 Hannover, Germany

Correspondence to: M. Kaliske

Dedicated to Prof. Dr.-Ing. W. Wunderlich, München, on the occasion of his sixty-fifth birthday.

The authors gratefully acknowledge the support of the Continental AG in providing experimental data and financial assistance.

Research and development in many engineering fields can be accelerated and optimized by numerical simulations. The study on hand provides a mathematical and numerical model for viscoelasticity which yields in combination with the finite element method an improved solution procedure for the mentioned class of design tasks.

Viscoelastic materials are distinguished from materials which are idealized as being purely elastic. They exhibit properties such as relaxation, creep and frequency-dependent stiffness and dissipative characteristics as well as strain-rate-dependent hysteretic behaviour. The appropriate mathematical model uses either a differential operator representation or a formulation utilizing convolution integrals. The latter approach is followed in this paper.

The fundamental theory of viscoelasticity is described in a number of textbooks such as Findley, Lai and Onaran (1976), Christensen (1982) and Aklonis and MacKnight (1983). A lot of articles is concerned with specific aspects or formulations and cannot be mentioned here in detail. We refer the interested reader to Morman (1985) who published a detailed review of finite elasticity as well as of linear and nonlinear viscoelastic theories.

Our article makes use of the work of Taylor, Pister and Goudreau (1970), where a numerical formulation based on a thermomechanical description for axisymmetric linear viscoelasticity at small strains is presented. They derived a convolution integral to take the total deformation history into account resulting in a recursive formula. Simo (1987), Govindjee and Simo (1992) and the formulation given here employ this approach to evaluate the history-dependent deformation.

The multiplicative split of the deformation gradient $\underline{\mathbf{F}} = J^{\frac{1}{3}}\underline{\mathbf{1}}\,\overline{\underline{\mathbf{F}}}^{e}\underline{\mathbf{F}}^{v}$ is of fundamental importance for another viscoelastic approach given by Lubliner (1985). The volumetric deformation $\underline{\mathbf{F}}_{vol} = J^{\frac{1}{3}}\underline{\mathbf{1}}$ is considered as being purely elastic. The isochoric part $\underline{\mathbf{F}}_{iso} = \overline{\underline{\mathbf{F}}}^{e}\underline{\mathbf{F}}^{v}$ is divided up multiplicatively into an elastic $\overline{\underline{\mathbf{F}}}^{e}$ and an inelastic portion $\underline{\mathbf{F}}^{v}$. This multiplicative separation for a viscoelastic formulation is already used by Sidoroff (1974). Lee (1969) introduced equivalent kinematic quantities for finite plasticity. Thus, he splits multiplicatively the deformation gradient $\underline{\mathbf{F}} = \underline{\mathbf{F}}^{e}\underline{\mathbf{F}}^{p}$ into an elastic $\underline{\mathbf{F}}^{e}$ and a plastic contribution $\underline{\mathbf{F}}^{p}$.

Both Lubliner (1985) and Simo (1987) propose a linear rate equation for internal stress variables of the 'standard-type' to define the viscoelastic model. Simo (1987) develops a finite isothermal and linear viscoelasticity combined with damage effects (see Mullins (1969)). The integration of the deformation history is accomplished by the recur-

rence relation of Taylor, Pister and Goudreau (1970) which has already been mentioned. The algorithm and the consistent linearized tangent operator are given by Simo in the reference configuration. Govindjee and Simo (1992) focus on damage phenomena in greater detail based on Simo (1987). Moreover, Im and Atluri (1987) published a paper on finite plasticity using an endochronic approach, which is essentially similar to viscoelasticity.

A generalized viscoelastic theory is proposed by Bagley and Torvik (1983). Padovan (1987) describes a finite element implementation of this model. Instead of integer time derivatives fractional order operators are introduced into the constitutive rate equation. For simulations in the time domain time consuming transformations are used to solve this extended formulation numerically. According to Bagley and Torvik less material parameters are required and a more flexible model is obtained compared to a constitutive approach using integer time derivatives. However, an extensive comparative study on this topic has not been published yet as far as the authors are aware.

The goal of this paper is the presentation of a compact and efficient three-dimensional viscoelastic formulation which is well suited for large scale finite element computations. It is based on the generalized Maxwell-element, i.e. a finite number of separate Maxwell-elements in parallel, and, therefore, it is valid for small and finite strains. This constitutive formulation has proved to be a realistic approach and, therefore, it is used frequently in polymer physics to describe rubber material. Moreover, the geometrical linear setting is readily extended to a nonlinear formulation. It may represent the basis for further extensions like thermo-viscoelasticity and damage phenomena which are not topic of the following considerations. The numerical model shown is linearized in closed form to yield a simple material tensor slightly different from an elastic model. Due to its simplicity the material tensor is determined directly in the current configuration for the large strain approach in the case of isotropy. After introducing the mathematical and the numerical model, aspects of the evaluation of experimental data and of parameter identification are addressed. Finally, the formulation is applied to finite element computations to show its efficiency and characteristics.

2
Phenomenological viscoelastic model

The derivation of the mathematical and the numerical viscoelastic model is performed in three steps. Firstly, the fundamental approach is given as a one-dimensional analytical description at small strain. Subsequently, the accompanying three-dimensional numerical formulation ready for a finite element implementation is given. It is followed by its geometrically nonlinear extension.

2.1
Basic formulation

The following development of a viscoelastic material formulation for solids is based on some fundamental assumptions. Thermorheologically simple materials for which the time-temperature superposition principle is valid (see Schwarzl and Staverman (1952)) are considered. The thermomechanically coupled process is simplified and the generation of heat is not taken into account, i.e., an isothermal situation is assumed. Furthermore, damage phenomena like the Mullins-effect (see Mullins (1969)) observed for rubber materials during the first loading cycles are not of interest in this study. We focus on linear viscoelastic material where the Boltzmann superposition principle is applicable.

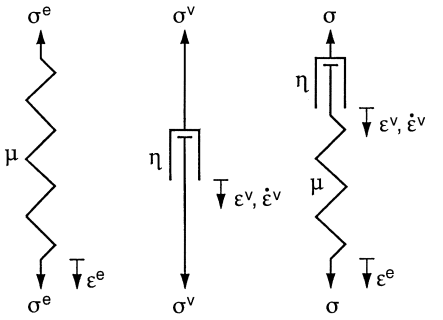

Fig. 1. Hooke-, Newton- and Maxwell-element

The developed viscoelastic formulation can be represented by a rheological analogy - the generalized Maxwell model - which is often used as a phenomenological approach to polymeric materials. Firstly, the derivations are given for one-dimensional, linear elastic and geometrically linear considerations.

The basic constitutive rheological elements of linear viscoelasticity are an elastic spring called Hooke-element and a viscous Newton-element (Fig. 1). The elastic material constant μ gives the linear relation

$$\sigma^e = \mu\epsilon^e \tag{1}$$

between elastic strain ϵ^e and elastic stress σ^e. The viscous stress σ^v of the Newton-element depends on the strain rate $\dot{\epsilon}^v$. For the Newton-element these quantities are related linearly by the coefficient of viscosity η

$$\sigma^v = \eta\dot{\epsilon}^v \tag{2}$$

analogously to the elastic Hooke-element. The viscosity η can also be expressed in terms of the elastic constant μ

$$\eta := \tau\mu \tag{3}$$

by introducing the relaxation time τ. Fig. 2 shows how the relaxation time τ is given by the initial slope of a relaxation test. The combination of Hooke- and Newton-element in series yields the so-called Maxwell-element (Fig. 1) where the total strain ϵ consists of an additive combination $\epsilon = \epsilon^e + \epsilon^v$ of an elastic ϵ^e and a viscous ϵ^v component while the stress

$$\sigma = \mu\epsilon^e = \eta\dot{\epsilon}^v \tag{4}$$

is, of course, in both rheological elements the same. From (4) $\dot{\epsilon}^v = \frac{1}{\tau}(\epsilon - \epsilon^v)$ can be obtained using $\epsilon^e = \epsilon - \epsilon^v$ and $\dot{\epsilon}^v = \frac{1}{\eta}\mu\epsilon^e$.

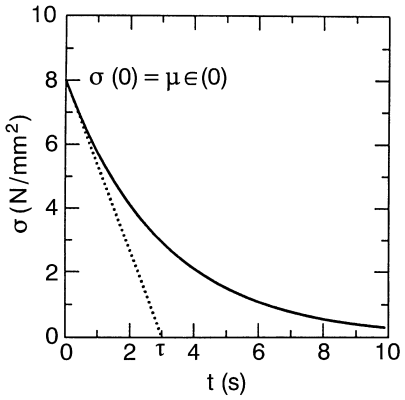

Fig. 2. Relaxation test of a Maxwell-element

At the state of equilibrium $\dot{\epsilon}^v = 0$ the viscous strain of a Maxwell-element converges to the total strain $\epsilon^v = \epsilon$ and the elastic strain vanishes $\epsilon^e = 0$. Alternatively, we get the fundamental differential equation

$$\dot{\epsilon} = \frac{1}{\mu}\dot{\sigma} + \frac{1}{\eta}\sigma \tag{5}$$

for the stress of a Maxwell-element from $\dot{\epsilon} = \dot{\epsilon}^e + \dot{\epsilon}^v$.

When carrying out a relaxation test (Fig. 2) a Maxwell-element is deformed $\hat{\epsilon}(0) = \hat{\epsilon}(t) = \text{const.}$ at a constant strain. In this case the solution of the differential equation (5) yields

$$\sigma_h = c\, \exp\left(-\frac{t}{\tau}\right) \text{ and } \sigma_p = 0 \tag{6}$$

for the homogeneous and the particular solution, respectively. By using the initial condition $\hat{\sigma}(0) = \mu\hat{\epsilon}(0)$ the constant $c = \mu\hat{\epsilon}(0)$ is determined. Thus, we get the solution

$$\hat{\sigma}(t) = \mu\, \exp\left(-\frac{t}{\tau}\right)\hat{\epsilon}(0) \tag{7}$$

where the relaxation function

$$\hat{\Gamma}(t) = \mu\, \exp\left(-\frac{t}{\tau}\right) \tag{8}$$

defines the specific viscoelastic characteristics of the material. At an infinite large time the stress is fully reduced $\hat{\sigma}(\infty) = 0$.

The preceding relaxation test of one Maxwell-element is easily applied to an extended viscoelastic formulation where a finite number of separate Maxwell-elements are arranged in parallel with an elastic Hooke-element (Fig. 3). The stress relaxation for the generalized Maxwell-element is given by

$$\begin{aligned}\hat{\sigma}(t) &= \mu_0\, \hat{\epsilon}(0) + \sum_{j=1}^{N} \mu_j\, \exp\left(-\frac{t}{\tau_j}\right)\hat{\epsilon}(0) \\ &= \hat{\Gamma}(t)\,\hat{\epsilon}(0)\end{aligned} \tag{9}$$

where

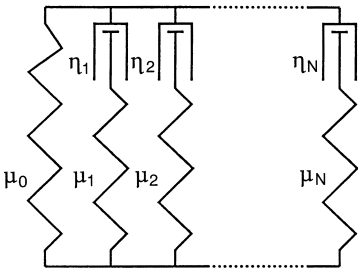

Fig. 3. Generalized Maxwell-element

$$\hat{\Gamma}(t) = \mu_0 + \sum_{j=1}^{N} \mu_j\, \exp\left(-\frac{t}{\tau_j}\right) \tag{10}$$

defines the characteristic relaxation function of N Maxwell-elements (Fig. 3). The time-independent elastic part of the deformation is represented by the term μ_0 which is constant with respect to time. In this paper the relaxation function (10) will be used in a normalized form. It is related to the elastic part μ_0. Thus, we introduce

$$\hat{\gamma}(t) = \frac{\hat{\Gamma}(t)}{\mu_0} = 1 + \sum_{j=1}^{N} \gamma_j\, \exp\left(-\frac{t}{\tau_j}\right)\ . \tag{11}$$

Viscoelastic formulations can be derived on the basis of either differential operators or convolution integrals as mentioned in the introduction. The latter approach is followed in this paper. Starting from the Boltzmann superposition principle a creep test is considered. A Maxwell-material is loaded at time $t \geq t_0$ by a constant stress σ_0. The strain is a function of time

$$\hat{\epsilon}_0(t) = \hat{\Upsilon}(t - t_0)\hat{H}(t - t_0)\sigma_0 \tag{12}$$

expressed by the creep function $\hat{\Upsilon}(t - t_0)$ and the Heaviside unit step function $\hat{H}(t - t_0)$. The rheological element is subjected to an additional stress σ_1 at $t \geq t_1$ which leads to an equivalent strain response. According to the Boltzmann superposition principle the response for the combined load history $i = 1, \ldots, M$

$$\hat{\sigma}(t) = \sum_{i=1}^{M} \hat{H}(t - t_i)\Delta\sigma_i \tag{13}$$

is computed directly by superposition of the separate responses

$$\hat{\epsilon}(t) = \sum_{i=1}^{M} \hat{\epsilon}_i(t - t_i) = \sum_{i=1}^{M} \hat{\Upsilon}(t - t_i)\hat{H}(t - t_i)\Delta\sigma_i \tag{14}$$

from the separate loadings $\Delta\sigma_i$ to give the combined result. When infinitesimal load steps $\Delta\sigma_i$ are applied, the total strain is determined by the integral representation

$$\hat{\epsilon}(t) = \int_0^t \hat{\Upsilon}(t - s)\hat{H}(t - s)\, \mathrm{d}\hat{\sigma}(s) \tag{15}$$

to sum up the deformation history. This hereditary integral is reduced to

$$\hat{\epsilon}(t) = \int_0^t \hat{\Upsilon}(t-s)\frac{\partial\sigma}{\partial s}\,\mathrm{d}s \tag{16}$$

when the stress history is differentiable with respect to time.

Analogous steps for the relaxation test yield an equivalent integral representation

$$\hat{\sigma}(t) = \int_0^t \hat{\Gamma}(t-s)\frac{\partial\epsilon}{\partial s}\,\mathrm{d}s \tag{17}$$

where $\hat{\Gamma}(t-s)$ is the relaxation function. Creep and relaxation are merely two different aspects of the phenomenon viscoelasticity. Therefore, the transition from one property to the other can be shown by Laplace- or Fourier-transformation (see Findley et al. (1976)).

Complex Moduli The relaxation and creep tests described characterize the behaviour of viscoelastic solids as a function of time. To understand the phenomena in greater detail and to compute the response of a dynamically loaded viscoelastic body, the material is subjected to an oscillating load resulting in a state of stress

$$\sigma = \sigma_0 \cos\omega t \tag{18}$$

which varies harmonically with frequency ω. The stress amplitude is σ_0. For the description of a harmonic vibration it is useful to represent the oscillation by a vector in the complex plane rotating about the origin. The transition from polar coordinates to Eulerian representation

$$\cos\omega t + i\sin\omega t = \exp(i\omega t) \tag{19}$$

yields

$$\sigma = \sigma_0 \exp(i\omega t) \tag{20}$$

where $i := \sqrt{-1}$. The accompanying strain response

$$\epsilon = \epsilon_0 \cos(\omega t - \delta) \quad \text{or} \quad \epsilon = \epsilon_0 \exp[i(\omega t - \delta)] \tag{21}$$

oscillates at the same frequency ω but lags behind the stress by the phase angle δ. This phase shift δ, often called loss angle, is an important quantity for the characterization of viscoelastic dissipative properties. The phase shift causes a hysteresis in the stress-strain diagram of a harmonic vibration. The area described by the hysteresis is a measure for the energy dissipated in one cycle of vibration.

We shall apply this frequency-dependent formulation to the generalized Maxwell-model. Reformulation of Eq. (5)

$$\mu\tau\,\dot{\epsilon} = \tau\,\dot{\sigma} + \sigma \tag{22}$$

and inserting the complex stress and strain quantities leads to

$$i\omega\tau\mu\,\epsilon_0 = \sigma_0 \exp(i\delta)\,(1 + i\omega\tau)\ . \tag{23}$$

This defines the complex relaxation modulus

$$\Gamma^* = \frac{\sigma_0}{\epsilon_0}\exp(i\delta) = \mu\frac{i\omega\tau}{1+i\omega\tau} \tag{24}$$

for one Maxwell-element. Splitting the complex quantity Γ^* into a real and an imaginary part

$$\Gamma^* = \Gamma' + i\,\Gamma'' = \mu\frac{\omega^2\tau^2}{1+\omega^2\tau^2} + i\,\mu\frac{\omega\tau}{1+\omega^2\tau^2} \tag{25}$$

results in the components Γ' and Γ'' called storage and loss modulus.

The mechanical loss factor as the ratio of imaginary Γ'' and real part Γ'

$$\tan\delta = \frac{\Gamma''}{\Gamma'} = \frac{1}{\omega\,\tau} \tag{26}$$

is also a function of the frequency like Γ' and Γ''. Similarly, the complex modulus for the generalized Maxwell-element is computed as

$$\begin{aligned}\Gamma^* &= \Gamma' + i\,\Gamma'' \\ &= \mu_0 + \sum_{j=1}^{N}\mu_j\frac{i\omega\tau_j}{1+i\omega\tau_j} \\ &= \mu_0 + \sum_{j=1}^{N}\mu_j\frac{\omega^2\tau_j^2}{1+\omega^2\tau_j^2} + i\sum_{j=1}^{N}\mu_j\frac{\omega\tau_j}{1+\omega^2\tau_j^2}\ ,\end{aligned} \tag{27}$$

for N viscous elements and an elastic spring μ_0 or as the normalized modulus

$$\begin{aligned}\gamma^* &= \gamma' + i\,\gamma'' \\ &= 1 + \sum_{j=1}^{N}\gamma_j\frac{i\omega\tau_j}{1+i\omega\tau_j} \\ &= 1 + \sum_{j=1}^{N}\gamma_j\frac{\omega^2\tau_j^2}{1+\omega^2\tau_j^2} + i\sum_{j=1}^{N}\gamma_j\frac{\omega\tau_j}{1+\omega^2\tau_j^2}\ .\end{aligned} \tag{28}$$

This complex relaxation function (27) and (28) can be derived directly by a Fourier-transform of the time-dependent function (10) and (11) from time domain to frequency domain.

2.2 Linear viscoelasticity

The development of a numerical model starts from the general integral representation of linear viscoelasticity

$$\begin{aligned}&\hat{\sigma}(t) = \int_0^t \hat{\Gamma}(t-s)\frac{\partial\hat{\epsilon}(s)}{\partial s}\,\mathrm{d}s \\ &\text{where}\quad \hat{\Gamma}(t-s) = \mu_0 + \sum_{j=1}^{N}\mu_j\exp\left(-\frac{t-s}{\tau_j}\right)\end{aligned} \tag{29}$$

as an one-dimensional formulation given by equation (Eq. (17)). Splitting the integral into an elastic and a viscoelastic contribution leads to

$$\begin{aligned}\hat{\sigma}(t) &= \int_0^t \mu_0 \frac{\partial \hat{\epsilon}(s)}{\partial s}\,\mathrm{d}s \\ &\quad + \int_0^t \sum_{j=1}^{N} \mu_j \exp\left(-\frac{t-s}{\tau_j}\right) \frac{\partial \hat{\epsilon}(s)}{\partial s}\,\mathrm{d}s \\ &= \mu_0 \hat{\epsilon}(t) + \sum_{j=1}^{N} \int_0^t \mu_j \exp\left(-\frac{t-s}{\tau_j}\right) \frac{\partial \hat{\epsilon}(s)}{\partial s}\,\mathrm{d}s \\ &= \hat{\sigma}_0(t) + \sum_{j=1}^{N} \hat{h}_j(t)\ , \end{aligned} \tag{30}$$

the elastic stress component $\hat{\sigma}_0(t)$ and the internal stress equivalent variables $\hat{h}_j(t)$. In a relaxation test the contribution of the internal variables $\hat{h}_j(t)$ to the state of stress vanishes

$$\lim_{t\to\infty} \hat{h}_j(t) = 0 \tag{31}$$

when time tends towards infinity. The goal of the following steps is to obtain an efficient numerical formulation for the solution of the hereditary integral

$$\hat{h}_j(t) = \int_0^t \mu_j \exp\left(-\frac{t-s}{\tau_j}\right) \frac{\partial \hat{\epsilon}(s)}{\partial s}\,\mathrm{d}s \tag{32}$$

for each separate history variable $\hat{h}_j(t)$. This convolution integral is derived from the linear rate equation

$$\dot{h}_j + \frac{1}{\tau_j} h_j = \gamma_j \dot{\sigma}_0 \tag{33}$$

for one Maxwell-element j, i.e. one internal stress variable h_j of the generalized rheological model. The rate equation (33) is based on the differential equation for the stress (5). Substituting the strain by $\hat{\epsilon}(t) = \frac{\hat{\sigma}_0(t)}{\mu_0}$ in (32) leads to

$$\hat{h}_j(t) = \int_0^t \gamma_j \exp\left(-\frac{t-s}{\tau_j}\right) \frac{\partial \hat{\sigma}_0(s)}{\partial s}\,\mathrm{d}s\ , \tag{34}$$

a representation of the internal variables in terms of the stress $\hat{\sigma}_0(t)$ and the factor γ_j of the normalized relaxation function. The efficient solution of this hereditary integral is crucial for a numerical implementation.

Considering the time interval $[t_n, t_{n+1}]$ we define the time step $\Delta t := t_{n+1} - t_n$. Utilizing a multiplicative split of the exponential expression

$$\begin{aligned}\exp\left(-\frac{t_{n+1}}{\tau_j}\right) &= \exp\left(-\frac{t_n + \Delta t}{\tau_j}\right) \\ &= \exp\left(-\frac{t_n}{\tau_j}\right) \exp\left(-\frac{\Delta t}{\tau_j}\right)\end{aligned} \tag{35}$$

and the separation of the deformation history into a period $0 \le s \le t_n$ when the result is known and into the current unknown time step $t_n \le s \le t_{n+1}$ yields

$$\begin{aligned}\hat{h}_j(t_{n+1}) &= \gamma_j \int_0^{t_{n+1}} \exp\left(-\frac{t_{n+1}-s}{\tau_j}\right) \frac{\mathrm{d}\hat{\sigma}_0(s)}{\mathrm{d}s}\,\mathrm{d}s \\ &= \exp\left(-\frac{\Delta t}{\tau_j}\right) \gamma_j \int_0^{t_n} \exp\left(-\frac{t_n - s}{\tau_j}\right) \frac{\mathrm{d}\hat{\sigma}_0(s)}{\mathrm{d}s}\,\mathrm{d}s \\ &\quad + \gamma_j \int_{t_n}^{t_{n+1}} \exp\left(-\frac{t_{n+1}-s}{\tau_j}\right) \frac{\mathrm{d}\hat{\sigma}_0(s)}{\mathrm{d}s}\,\mathrm{d}s \\ &= \exp\left(-\frac{\Delta t}{\tau_j}\right) \hat{h}_j(t_n) \\ &\quad + \gamma_j \int_0^{t_{n+1}} \exp\left(-\frac{t_{n+1}-s}{\tau_j}\right) \frac{\mathrm{d}\hat{\sigma}_0(s)}{\mathrm{d}s}\,\mathrm{d}s\end{aligned} \tag{36}$$

an exact recursive formula for the current value of the stress quantity h_j. The transition from differential coefficient to discrete time steps

$$\frac{\mathrm{d}\hat{\sigma}_0(s)}{\mathrm{d}s} = \lim_{\Delta s\to 0} \frac{\Delta \hat{\sigma}_0(s)}{\Delta s} = \lim_{\Delta t\to 0} \frac{\sigma_0^{n+1} - \sigma_0^n}{\Delta t} \tag{37}$$

introduces a time approximation of second order into the formula which was exact so far. The remaining expression

$$\begin{aligned}h_j^{n+1} &= \exp\left(-\frac{\Delta t}{\tau_j}\right) h_j^n \\ &\quad + \gamma_j \int_{t_n}^{t_{n+1}} \exp\left(-\frac{t_{n+1}-s}{\tau_j}\right) \mathrm{d}s \frac{\sigma_0^{n+1} - \sigma_0^n}{\Delta t}\end{aligned} \tag{38}$$

is integrated analytically. We end up with a recursive formula

$$h_j^{n+1} = \exp\left(-\frac{\Delta t}{\tau_j}\right) h_j^n + \gamma_j \frac{1 - \exp\left(-\frac{\Delta t}{\tau_j}\right)}{\frac{\Delta t}{\tau_j}} [\sigma_0^{n+1} - \sigma_0^n] \tag{39}$$

for an update of the stress variables given in a similar manner already by Herrmann and Peterson (1968) as well as by Taylor, Pister and Goudreau (1970). The recursive determination of the current variables h_j^{n+1} requires the quantities σ_0^n, h_j^n where $j = 1, \ldots, N$ of the preceding time step n and, therefore, they have to be stored in a data base. The shown strain-driven integration algorithm is unconditionally stable for small and large time steps and it is second order accurate.

A crucial aspect of the implementation of the integration algorithm is its consistent linearization. The one-dimensional viscoelastic tangent modulus

$$C^{v,n+1} := \frac{\partial \sigma^{n+1}}{\partial \epsilon^{n+1}} = \left\{ 1 + \sum_{j=1}^{N} \gamma_j \frac{1 - \exp\left(-\frac{\Delta t}{\tau_j}\right)}{\frac{\Delta t}{\tau_j}} \right\} \mu_0 \tag{40}$$

is computed as the derivative of the current state of stress

$$\sigma^{n+1} = \mu_0 \epsilon^{n+1} + \sum_{j=1}^{N} h_j^{n+1} \tag{41}$$

with respect to the current strain ϵ^{n+1}. We end up with a constant algorithmic tangent modulus $C^{v,n+1}$ for a constant elastic quantity μ_0 and an unchanged time step Δt.

The extension of the shown formulation to a fully three-dimensional approach is easily performed by introducing tensor quantities. The total stresses of a linear elastic Maxwell-material

$$\underline{\boldsymbol{\sigma}}^{n+1} = \underline{\boldsymbol{\sigma}}_0^{n+1} + \sum_{j=1}^{N} \underline{\mathbf{h}}_j^{n+1} \tag{42}$$

are determined from the elastic contribution

$$\underline{\boldsymbol{\sigma}}_0^{n+1} = \underline{\underline{\mathbb{C}}}^e \underline{\boldsymbol{\epsilon}}^{n+1} \tag{43}$$

and from internal stress variables

$$\underline{\mathbf{h}}_j^{n+1} = \exp\left(-\frac{\Delta t}{\tau_j}\right)\underline{\mathbf{h}}_j^n + \gamma_j \frac{1-\exp\left(-\frac{\Delta t}{\tau_j}\right)}{\frac{\Delta t}{\tau_j}}\left[\underline{\boldsymbol{\sigma}}_0^{n+1} - \underline{\boldsymbol{\sigma}}_0^n\right] \tag{44}$$

which are described by second order tensors. The material parameter γ_j is still employed as a scalar quantity in the underlying constitutive rate equation for the three-dimensional extension

$$\dot{\underline{\mathbf{h}}}_j + \frac{1}{\tau_j}\underline{\mathbf{h}}_j = \gamma_j \dot{\underline{\boldsymbol{\sigma}}}_0 \tag{45}$$

and equivalently in the geometrical nonlinear setting (53). Therefore, the model shown is restricted to isotropy. In the general case, e.g. when orthotropic material is considered, this quantity has to be represented by an unsymmetric fourth order tensor $\underline{\underline{\boldsymbol{\gamma}}}_j$.

The analytical linearization, i.e. the algorithmic material tensor,

$$\underline{\underline{\mathbb{C}}}^{v,n+1} := \frac{\partial \underline{\boldsymbol{\sigma}}^{n+1}}{\partial \underline{\boldsymbol{\epsilon}}^{n+1}} = \left\{1 + \sum_{j=1}^{N} \gamma_j \frac{1-\exp\left(\frac{\Delta t}{\tau_j}\right)}{\frac{\Delta t}{\tau_j}}\right\} \underline{\underline{\mathbb{C}}}^{e,n+1} \tag{46}$$

is computed analogously to the one-dimensional formulation by the scalar quantity

$$1 + \sum_{j=1}^{N} \gamma_j \frac{1-\exp\left(-\frac{\Delta t}{\tau_j}\right)}{\frac{\Delta t}{\tau_j}} \quad , \tag{47}$$

which takes the viscoelastic characteristics into account, and by the constant elasticity tensor $\underline{\underline{\mathbb{C}}}^e$ in case of linear Hooke-material. The stress tensors $\underline{\boldsymbol{\sigma}}_0^n$, $\underline{\mathbf{h}}_j^n$, where $j = 1, \ldots, N$ need to be stored in a data base for the recursive update of the stress quantities at the next time step $n+1$.

Experimental investigations have shown that in many cases viscoelastic behaviour is mainly related to the isochoric part of the deformation. Thus, the volume dilatation is considered as being purely elastic. In contrast to total viscoelasticity introduced before, a volumetric and isochoric split of the stresses is required to formulate separate material properties. The stresses for an isochoric viscoelastic model

$$\underline{\boldsymbol{\sigma}}^{n+1} = \kappa \, \mathrm{I}_{\underline{\boldsymbol{\epsilon}}}^{n+1} \underline{\mathbf{1}} + \mathrm{dev}\, \underline{\boldsymbol{\sigma}}^{n+1} \tag{48}$$

are composed of elastic hydrostatic pressure where κ is the bulk modulus and the viscoelastic deviatoric part

$$\mathrm{dev}\, \underline{\boldsymbol{\sigma}}^{n+1} = \mathrm{dev}\, \underline{\boldsymbol{\sigma}}_0^{n+1} + \sum_{j=1}^{N} \underline{\mathbf{h}}_j^{n+1} \tag{49}$$

of the stresses. For the computation of the history variables

$$\begin{aligned}\underline{\mathbf{h}}_j^{n+1} = &\exp\left(-\frac{\Delta t}{\tau_j}\right)\underline{\mathbf{h}}_j^n \\ &+ \gamma_j \frac{1-\exp\left(-\frac{\Delta t}{\tau_j}\right)}{\frac{\Delta t}{\tau_j}}\left[\mathrm{dev}\, \underline{\boldsymbol{\sigma}}_0^{n+1} - \mathrm{dev}\, \underline{\boldsymbol{\sigma}}_0^n\right]\end{aligned} \tag{50}$$

deviatoric stress tensors only are taken into account. The tangential algorithmic material tensor

$$\begin{aligned}\underline{\underline{\mathbb{C}}}^{v,n+1} =& \underline{\underline{\mathbb{C}}}_{vol}^{e,n+1} + \left\{1 + \sum_{j=1}^{N} \gamma_j \frac{1-\exp\left(-\frac{\Delta t}{\tau_j}\right)}{\frac{\Delta t}{\tau_j}}\right\} \underline{\underline{\mathbb{C}}}_{iso}^{e,n+1} \\ =& \kappa\, (\underline{\mathbf{1}} \otimes \underline{\mathbf{1}}) + \left\{1 + \sum_{j=1}^{N} \gamma_j \frac{1-\exp\left(-\frac{\Delta t}{\tau_j}\right)}{\frac{\Delta t}{\tau_j}}\right\} \\ &\times 2\mu_0 \left[\underline{\underline{\mathbf{I}}} - \frac{1}{3}(\underline{\mathbf{1}} \otimes \underline{\mathbf{1}})\right]\end{aligned} \tag{51}$$

is split in a similar way and the viscoelastic approach is applied only to the isochoric term.

2.3 Finite viscoelasticity

An extension of the presented formulation to finite strains is easily accomplished because the generalized Maxwell-element is chosen as the underlying viscoelastic material structure. The rheological elements in parallel preserve the linear structure of the formulation even for the generalized Maxwell-material at finite strains.

The basis for the shown isochoric finite viscoelasticity is a determination of deviatoric stresses in the reference configuration (see Eq. (67) for the definition of DEV $(\bullet)$)

$$\mathrm{DEV}\, \underline{\mathbf{S}}^{n+1} = \mathrm{DEV}\, \underline{\mathbf{S}}_0^{n+1} + \sum_{j=1}^{N} \underline{\mathbf{H}}_j^{n+1} \tag{52}$$

which are the elastic and viscoelastic parts of the second Piola-Kirchhoff stress tensor. The description in the reference configuration is required in order to preserve the principle of objectivity. Based on the linear rate equation for the internal stress variables $\underline{\mathbf{H}}_j$

$$\dot{\underline{\mathbf{H}}}_j + \frac{1}{\tau_j}\underline{\mathbf{H}}_j = \gamma_j \mathrm{DEV}\ \dot{\underline{\mathbf{S}}}_0 \tag{53}$$

the convolution integral and, subsequently, the recurrence relation

$$\begin{aligned}\underline{\mathbf{H}}_j^{n+1} &= \gamma_j \int_0^{t_{n+1}} \exp\left(-\frac{t_{n+1}-s}{\tau_j}\right) \frac{\mathrm{d}\,\mathrm{DEV}\ \hat{\underline{\mathbf{S}}}_0(s)}{\mathrm{d}s}\,\mathrm{d}s \\ &\approx \exp\left(-\frac{\Delta t}{\tau_j}\right)\underline{\mathbf{H}}_j^n \\ &\quad + \gamma_j \frac{1-\exp\left(-\frac{\Delta t}{\tau_j}\right)}{\frac{\Delta t}{\tau_j}}\left[\mathrm{DEV}\,\underline{\mathbf{S}}_0^{n+1} - \mathrm{DEV}\,\underline{\mathbf{S}}_0^n\right]\end{aligned} \tag{54}$$

for the stress update are derived. The formulation for finite strains is developed by analogous steps as for small strains in the preceding subsection. Similarly to the geometrically linear case already shown, the stress quantities $\mathbf{DEV}\ \underline{\mathbf{S}}_0^n, \underline{\mathbf{H}}_j^n$ where $j = 1, \ldots, N$ of the nonlinear elastic large strain model have to be stored throughout one time step. A push-forward transformation of the second Piola-Kirchhoff stress tensor utilizing the current deformation gradient $\underline{\mathbf{F}}^{n+1}$

$$\mathrm{dev}\ \underline{\boldsymbol{\tau}}^{n+1} = \Phi(\mathrm{DEV}\ \underline{\mathbf{S}}^{n+1})_* = \underline{\mathbf{F}}^{n+1}\mathrm{DEV}\ \underline{\mathbf{S}}^{n+1}(\underline{\mathbf{F}}^{n+1})^T \tag{55}$$

yields the Kirchhoff stresses in the current configuration. Thus, the total stress tensor

$$\underline{\boldsymbol{\tau}}^{n+1} = J^{n+1}U'^{\,n+1}\underline{\mathbf{1}} + \mathrm{dev}\ \underline{\boldsymbol{\tau}}^{n+1} \tag{56}$$

is composed of the elastic hydrostatic pressure and the computed viscoelastic deviatoric part. In Eq. (56) $\hat{U}(J)$ denotes the volumetric strain energy function which is given in terms of the Jacobian J. The derivative with respect to J is indicated by $U' = \frac{\mathrm{d}U}{\mathrm{d}J}$.

The algorithmic material tensor has its central significance especially for the solution procedure of a nonlinear system to equations when using a Newton algorithm. It results in a quadratic rate of convergence at least in the neighbourhood of the solution. The tangent modulus is computed as the linearization of the stress integration procedure, i.e. the derivative of the stress tensor with respect to the right Cauchy-Green strain tensor

$$\underline{\underline{\mathbb{C}}}_{iso}^{v,n+1} := 2\frac{\partial \underline{\mathbf{S}}_{iso}^{n+1}}{\partial \underline{\mathbf{C}}^{n+1}} = \left\{1 + \sum_{j=1}^{N}\gamma_j \frac{1-\exp\left(-\frac{\Delta t}{\tau_j}\right)}{\frac{\Delta t}{\tau_j}}\right\}\underline{\underline{\mathbb{C}}}_{iso}^{e,n+1} \tag{57}$$

and yields a fourth order material tensor in the reference configuration. From (57) the important conclusion can be drawn that the structure of the viscoelastic material tensor $\underline{\underline{\mathbb{C}}}_{iso}^{v,n+1}$ for the algorithm shown is similar to the accompanying elastic tensor $\underline{\underline{\mathbb{C}}}_{iso}^{c,n+1}$ which is merely modified by a scalar quantity. This result leads to a very efficient numerical implementation of the viscoelastic formulation. Moreover, it is possible to form the viscoelastic tangent $\underline{\underline{\mathbb{C}}}_{iso}^{v,n+1}$ directly in the current configuration

$$\begin{aligned}\underline{\underline{\mathbb{C}}}_{iso}^{v,n+1} &= \Phi\left(\underline{\underline{\mathbb{C}}}_{iso}^{v,n+1}\right)_* \\ &= \left\{1 + \sum_{j=1}^{N}\gamma_j \frac{1-\exp\left(-\frac{\Delta t}{\tau_j}\right)}{\frac{\Delta t}{\tau_j}}\right\}\Phi\left(\underline{\underline{\mathbb{C}}}_{iso}^{e,n+1}\right)_* \\ &= \left\{1 + \sum_{j=1}^{N}\gamma_j \frac{1-\exp\left(-\frac{\Delta t}{\tau_j}\right)}{\frac{\Delta t}{\tau_j}}\right\}\underline{\underline{\mathbb{C}}}_{iso}^{e,n+1}\end{aligned} \tag{58}$$

and to avoid time-consuming push-forward transformations by the deformation gradient $\Phi(\underline{\underline{\mathbb{C}}}_{iso}^{v,n+1})_*$. Therefore, the constitutive rate equation reads

$$L_v(\underline{\boldsymbol{\tau}}) = \underline{\underline{\mathbb{C}}}^v : \underline{\mathbf{d}} \tag{59}$$

as the Lie-derivative of the Kirchhoff stress tensor with the rate of deformation tensor $\underline{\mathbf{d}}$ and the total tangent operator for an isochoric viscoelasticity

$$\underline{\underline{\mathbb{C}}}^{v,n+1} = \underline{\underline{\mathbb{C}}}_{vol}^{e,n+1} + \left\{1 + \sum_{j=1}^{N}\gamma_j \frac{1-\exp\left(-\frac{\Delta t}{\tau_j}\right)}{\frac{\Delta t}{\tau_j}}\right\}\underline{\underline{\mathbb{C}}}_{iso}^{e,n+1} \tag{60}$$

in the current configuration. It is given as an important result of this subsection. The analogy of the elastic (74) and the viscoelastic tangent modulus (58) is restricted only to the principal structure of these fourth order tensors because the contribution of the viscoelastic stress tensor $\underline{\boldsymbol{\tau}}^{n+1}$ (56) to $\underline{\underline{\mathbb{C}}}_{iso}^{e,n+1}$ (60) (see Eq. (74) for the general form) is determined through the integration of the material history (Eqs. (52) to (56)). Only in case of a hyperelastic approach the stresses $\underline{\boldsymbol{\tau}}$ are computed directly from a strain energy function (Eq. 71).

3 Experimental investigations

After having introduced the mathematical and the numerical model, some aspects of experimental evaluation and parameter identification will be considered in the following subsections.

3.1 Time-temperature superposition principle

In this paper we are looking at thermorheologically simple materials and, therefore, the time-temperature correspondence principle is applicable. Its fundamental idea is

that time and temperature have an equivalent influence on viscoelastic properties of polymers: an increasing temperature corresponds to an extension of the time scale of the experiment or to a decreased load frequency in a dynamic experiment. Conducting measurements at various temperatures can be interpreted as an affinitive shift of the modulus-time or modulus-frequency diagram along the time or frequency axis. The correspondence principle is formulated mathematically for a modulus M as

$$\hat{M}(T_1, t) = \hat{M}\left(T_2, \frac{t}{a_T}\right) \tag{61}$$

at two different temperatures T_1, T_2 and time t. In (61) frequency ω and time t have an equivalent meaning, but it has to be pointed out that frequency is a reciprocal time quantity. The correspondence principle postulates the existence of a corresponding data with the same value M at temperature T_2 for measured modulus M at temperature T_1, but at a different time quantity t and ω, respectively. In (61) a_T is the factor to shift the modulus M along the time scale according to the temperature increment $\Delta T = T_2 - T_1$. Fig. 4 illustrates the shifting of a fictitious series of experimental data. Here, results of a relaxation experiment in the time interval $t_1 < t < t_2$ are plotted in logarithmic scales for the modulus M which is determined at different temperatures $T_1 < T_2 < T_3 < T_4$. The correspondence principle provides the means to transform the experimental data to a continuous material curve at a constant temperature T_1.

3.2 WLF-equation

Williams, Landel and Ferry (1955) introduced a quantitative relation for the correspondence principle named after them. The shifting factor a_t is given explicitly by

$$\log a_T = -\frac{17.4\ (T - T_G)}{51.6 + (T - T_G)} \tag{62}$$

in a nearly universal manner. The constants 17.4, 51.6 vary slightly for different polymers and the only material constant required is the glass transition temperature T_G serving as a reference temperature. This relation (62) is based on the 'free volume theory' (see e.g. Eisele (1990)). Generally, the validity of the WLF-equation is indicated in the range of

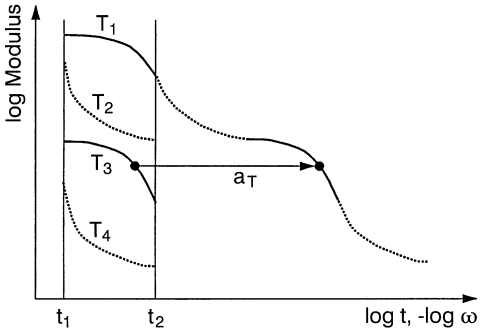

Fig. 4. Time-temperature superposition principle

$$T_G < T < T_G + 100 \tag{63}$$

in degrees Celsius.

3.3 Master-curves

In carrying out structural analyses, material moduli are needed over a large time scale or frequency scale. For technical reasons, the data are determined only within a limited range. But these measurements are performed at different temperatures. The experimentally determined material curves are shifted using the time-temperature correspondence principle, to give a continuous graph over a large time scale, the so-called master-curve. This frequency-dependent representation is a standard form in polymer physics. An inverse Fourier-transform of the complex modulus

$$\mathscr{F}^{-1}[\hat{\gamma}^*(\omega) = \hat{\gamma}'(\omega) + i\hat{\gamma}''(\omega)] = \hat{\gamma}(t) \tag{64}$$

would yield the accompanying diagram in the time domain. Generally, master-curves are utilized in the parameter-identification procedure.

The investigation on hand approximates the transformed data by an analytical fourth order polynomial. The coefficients of the terms are chosen by the least squares method. Usually, these material curves are given in terms of frequency.

Figure 5 shows that real part γ' and the imaginary part γ'' of a normalized complex relaxation modulus γ^* for a certain rubber material. The broken lines represent the transformed experimental data while the solid curve depicts its polynomial approximation. Both moduli γ', γ'' are strongly frequency-dependent for the material considered here, i.e. stiffness and damping characteristics vary with frequency ω at which an oscillation occurs.

3.4 Parameter-identification

After having introduced the mathematical and the numerical model and, subsequently, having commented on experimentally determined characteristics, the model has to be identified with the measured quantities. We make use of the generalized Maxwell-element and, thus, the constitutive quantities to be chosen are μ_j, τ_j (see Eq. (27)).

A large number of papers on this topic have been published. Among others Baumgaertel and Winter (1989) as well as Emri and Tschoegl (1993) developed algorithms to fit the mathematical model to measured data. Here, a collocation method mentioned by Tschoegl (1989) is taken to determine constitutive parameters. This simple and pragmatic procedure yields the constitutive data. An assessment of the experimental results and a deeper insight into the mathematical model could bring sophisticated identification methods used e.g. by Mahnken and Stein (1994) which represent a large field of research.

The shifted and smoothed data of Fig. 5 are approximated by Maxwell-elements, equally distributed along the logarithmic frequency axis (see Fig. 6). The contributions

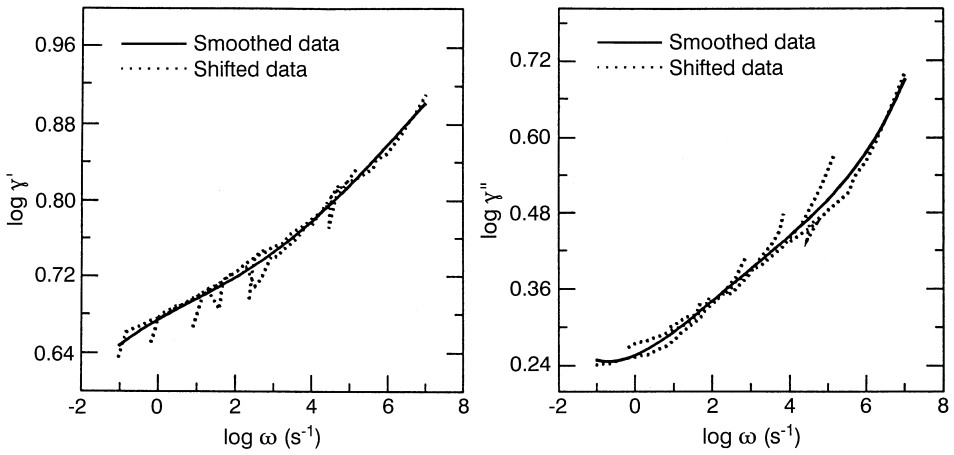

Fig. 5. Master-curves, shifted and smoothed data

of separate rheological elements, the cumulative curve and smoothed experimental data are plotted. Only for simplicity the material parameters have been chosen on the basis of the loss modulus γ'' in this case. Therefore, discrepancies between experiment and model curve are found for the storage modulus γ'. The deviation of measured data and mathematical approximation could e.g. alternatively be distributed to both the real and the imaginary part when a refined identification algorithm is used.

4
Numerical examples

In this section, numerical examples are presented to illustrate the characteristics of the material formulation and to show the good performance of the algorithm.

Example 4.1. The viscoelastic model is tested by uniaxial geometrically linear and linear elastic simulations using a 50 mm long sample discretized by one tri-linear finite element. The constitutive parameters of the generalized Maxwell-element consisting of 14 separate rheological elements in parallel are chosen according to the material given in Fig. 6. The specimen is excited by a step function $F(0) = F(t) = \text{const.}$ which starts oscillating about an equilibrium position. Large amplitudes are rapidly reduced and the dynamic response converges against the state of equilibrium (Fig. 7). The envelope of this viscously damped free-vibration test is an exponential curve which can clearly be seen.

Further characteristics of dissipative materials are explained in a path-controlled extension-compression test. The sample is subjected to a cyclic deformation up to a maximum of $\epsilon = \pm 10\%$. The load-deflection curve exhibits a hysteresis (Fig. 8) which is a measure for the energy dissipated within one cycle of loading. If the deformation is carried out at different periods T, i.e. at different strain rates $\dot{\epsilon}$, the slope of the hysteresis increases or decreases. This effect has its roots in the frequency-dependent stiffness of viscoelastic materials (see Fig. 6). Similarly, a frequency-dependent loss factor $\tan\delta$ is found.

Example 4.2. Half of a 50 mm long nearly incompressible ($\nu = 0.4995$) rubber cylinder is modelled by 54 tri-quadratic mixed brick-elements (according to the formulation of Simo and Taylor (1991)). The specimen has fixed boundary conditions at the top and is attached to a stiff steel plate at the bottom. This steel plate is loaded by a constant force F. The viscoelastic constants are chosen

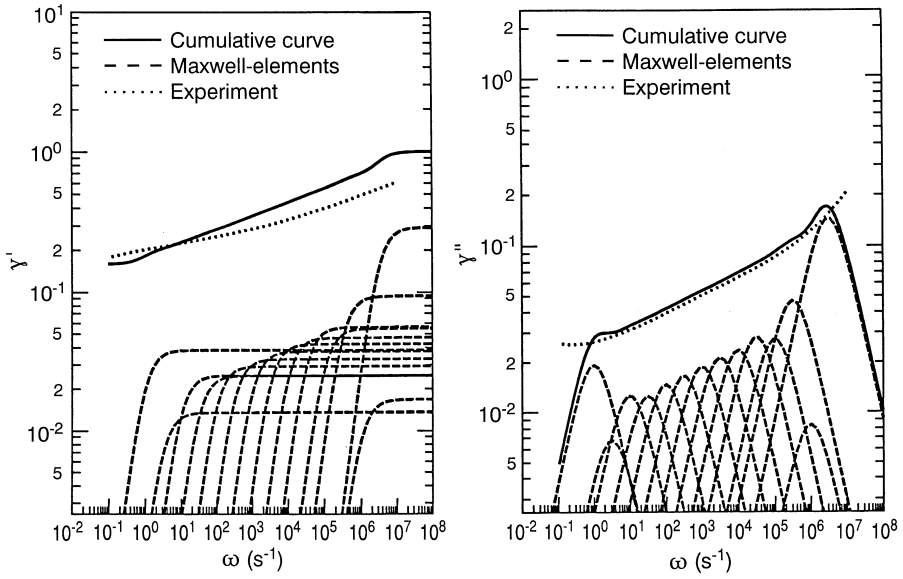

Fig. 6. Master-curves, experimental data and mathematical model

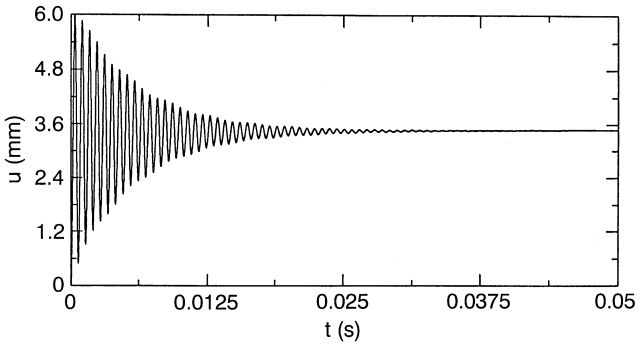

Fig. 7. Free-vibration test

according to Fig. 6. In contrast to example 4.1, the contribution of the elastic spring is neglected, i.e. $\gamma_0 = 0$, to yield a softer material.

Fig. 9 shows the state of deformation at different times t of this creep test. Maxwell-elements with short relaxation times τ_j deform fast at the beginning of the simulation and the creep process slows down with represent to time.

Example 4.3. A particular challenge for "computational mechanics" is the finite element analysis of tires. A variety of difficult topics are involved, such as nearly incompressible material, very stiff reinforcing fibres and elastic and inelastic properties of rubber material. As an example relevant to an industrial application, the dynamically excited cutout of a tire tread is considered (Fig. 10).

The local phenomena of a vibrating tire tread can be studied using a cutout which is modelled exactly through the thickness. Merely the dimensions in the tread plane are restricted. The admissibility of this model reduction is investigated by Jagusch, Kaliske and Rothert. The employed discretization is divided up into 208 mixed brick-elements with quadratic shape functions. Orthotropic fibre layers are represented by 128 membrane-elements.

The reduced tread model is used to simulate vibrations. Perpendicular to the surface the sample is excited by a step load $F(0) = F(t) = 10$ N. The model is composed of isotropic rubber layers idealized by the Neo-Hooke model and orthotropic membranes according to the de St. Venant-Kirchhoff approach. Making use of a second description, the elastic model is extended by the viscoelastic approach. The viscoelastic constitutive parameters are identified by using master-curves for the different rubber components.

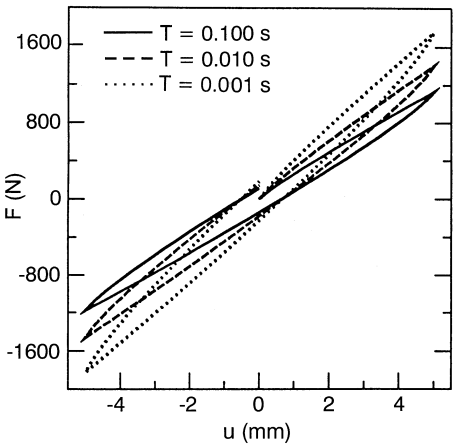

Fig. 8. Cyclic test

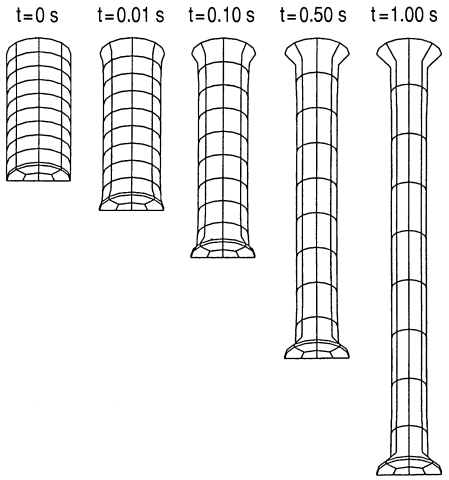

Fig. 9. Creep test

The plots in Fig. 11 depict the response u of the area where the load is applied as a function of time. The geometrically and physically nonlinear computations were carried out for an elastic and a viscoelastic modelling. The elastic response is characterized by an oscillation about the state of equilibrium which is superimposed by a large number of harmonic vibrations. The result is different when the viscoelastic model is applied. The excited area vibrates at a dominating frequency of approximately $f = 850$ Hz. Contributions of high frequency are also found. But the amplitudes are strongly damped so that the vibration changes over into a viscous relaxation process.

5 Conclusions

A generalized Maxwell-model is derived from basic considerations. To formulate the elastic component, any elastic constitutive approach is suitable. Certain emphasis is given to a volumetric-isochoric split of the deformation and, here, the isochoric part is related to the viscoelastic model. This constitutive assumption is confirmed by experiments and is valid for a large number of materials.

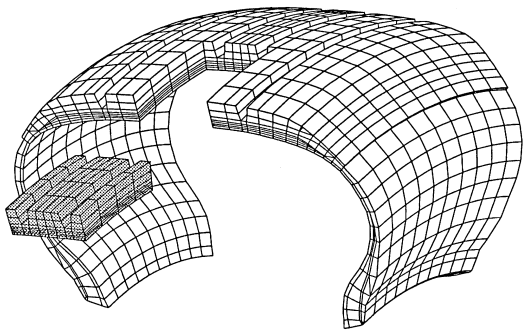

Fig. 10. Tire segment and tread cutout

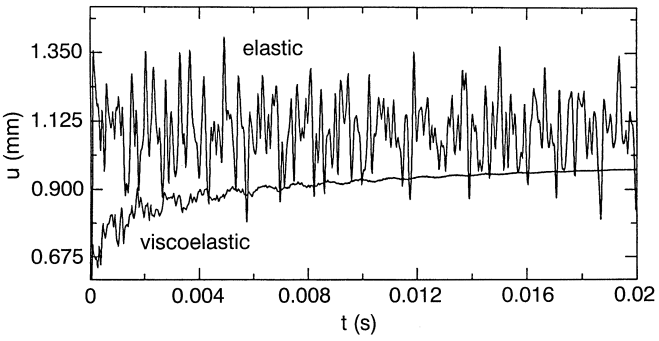

Fig. 11. Free-vibration test of a tire tread

It is shown that the main theoretical and numerical aspects of this geometrically linear and nonlinear viscoelastic formulation are identical. A stress-update in the reference configuration is necessary for finite viscoelasticity to fulfil the principle of objectivity. The symmetrical material operator can be derived analytically as a linearization of the stress integration algorithm. No restriction to the reference configuration is required for the computation of the material tensors in the case of isotropic elastic properties at finite strains.

The description is completed by comments on experimental evaluations and on parameter identification to put the mathematical and numerical model into practice. The combination of the viscoelastic approach we have presented with the finite element method provides an efficient numerical tool for large scale computations of time- and frequency-dependent materials.

Appendix

A
Definitions

The definition of the deviator of a second order tensor $(\underline{\bullet})$ in the current configuration is given by

$$\operatorname{dev}\,(\underline{\bullet}) := (\underline{\bullet}) - \frac{1}{3}\operatorname{tr}\,(\underline{\bullet})\underline{\mathbf{1}} \tag{65}$$

and the deviator of a fourth order tensor $(\underline{\underline{\bullet}})$ in the current configuration is

$$\begin{aligned}\operatorname{dev}(\underline{\underline{\bullet}}) :=& (\underline{\underline{\bullet}}) - \frac{1}{3}\underline{\mathbf{1}} \otimes [(\underline{\underline{\bullet}}) : \underline{\mathbf{1}}] - \frac{1}{3}[(\underline{\underline{\bullet}}) : \underline{\mathbf{1}}] \otimes \underline{\mathbf{1}} \\ &+ \frac{1}{9}[\underline{\mathbf{1}} : (\underline{\underline{\bullet}}) : \underline{\mathbf{1}}]\underline{\mathbf{1}} \otimes \underline{\mathbf{1}}\end{aligned} \tag{66}$$

where $\underline{\mathbf{1}}$ is a second order unit tensor. In the reference configuration the deviator of a second order tensor according to

$$\operatorname{DEV}(\underline{\bullet}) := (\underline{\bullet}) - \frac{1}{3}[\underline{\mathbf{C}} : (\underline{\bullet})]\underline{\mathbf{C}}^{-1} \tag{67}$$

is used where $\underline{\mathbf{C}}^{-1}$ is the inverse of the right Cauchy-Green tensor.

B
Finite elasticity

A brief representation of finite elasticity in the current configuration is shown for a better understanding of the viscoelastic approach. The accompanying elastic formulation in the reference configuration is easily obtained. Further details concerning finite elasticity are presented e.g. by Simo and Taylor (1991), van den Bogert and de Borst (1994) and Miehe (1994). Atluri and Reissner (1989) discuss in detail the volumetric and isochoric kinematic split (see e.g. equation (69)) as well as variational theorems for incompressible and nearly incompressible elasticity.

A fundamental kinematic quantity to describe deformation is the deformation gradient $\underline{\mathbf{F}}$. It defines the symmetrical right Cauchy-Green tensor $\underline{\mathbf{C}} := \underline{\mathbf{F}}^T\underline{\mathbf{F}}$ and the symmetrical left Cauchy-Green tensor $\underline{\mathbf{b}} := \underline{\mathbf{F}}\,\underline{\mathbf{F}}^T$. By linearization of the Lagrangian strain tensor $\underline{\mathbf{E}} = \frac{1}{2}(\underline{\mathbf{C}} - \underline{\mathbf{G}})$ where $\underline{\mathbf{G}}$ is the metric tensor in the reference configuration the small strain measure $\underline{\boldsymbol{\epsilon}} := \underline{\mathbf{E}}_{lin}$ is obtained. On the basis of strain tensor invariants e.g. for $\underline{\mathbf{b}}$

$$\begin{aligned}\mathrm{I}_{\underline{\mathbf{b}}} &= \operatorname{tr}\,\underline{\mathbf{b}} \\ \mathrm{II}_{\underline{\mathbf{b}}} &= \frac{1}{2}(\operatorname{tr}^2\,\underline{\mathbf{b}} - \operatorname{tr}\,\underline{\mathbf{b}}^2) \\ \mathrm{III}_{\underline{\mathbf{b}}} &= \det\,\underline{\mathbf{b}} = J^2\end{aligned} \tag{68}$$

constitutive elastic models are formulated.

In the context of this study the deformation gradient is splitted multiplicatively

$$\underline{\mathbf{F}} = (J^{\frac{1}{3}}\underline{\mathbf{1}})\overline{\underline{\mathbf{F}}} \tag{69}$$

which goes back to Flory (1961) to yield a volume-preserving part $\underline{\mathbf{F}}_{iso} = \overline{\underline{\mathbf{F}}}$ ($\det\,\overline{\underline{\mathbf{F}}} \equiv 1$) and the volumetric deformation $\underline{\mathbf{F}}_{vol} = J^{\frac{1}{3}}\underline{\mathbf{1}}$($\det\,\underline{\mathbf{F}} = J$). With this quantity at hand we define e.g. the volume-preserving part $\overline{\underline{\mathbf{b}}} = \overline{\underline{\mathbf{F}}}\,\overline{\underline{\mathbf{F}}}^T$ of the left Cauchy-Green tensor.

The elastic and inelastic properties of a certain material often exhibit different behaviour with respect to volumetric or deviatoric deformations. This phenomenon is taken into account by applying an additive split of the strain energy function

$$\boldsymbol{\Psi} = \hat{U}(J) + \hat{W}(\mathrm{I}_{\overline{\underline{\mathbf{b}}}}, \mathrm{II}_{\overline{\underline{\mathbf{b}}}}) \tag{70}$$

as the constitutive basis of the elastic properties. The first part U is a function of the volume-change J while the second term W is determined by the invariants $\mathrm{I}_{\overline{\underline{\mathbf{b}}}}, \mathrm{II}_{\overline{\underline{\mathbf{b}}}}$ of the volume-preserving part of the left Cauchy-Green tensor $\overline{\underline{\mathbf{b}}}$. Instead of an invariant based function a formulation in terms of principal stretches could be employed (see e.g. Ogden 1982).

The Kirchhoff stress tensor $\underline{\boldsymbol{\tau}}$ and the accompanying material tensor in the current configuration $\underline{\underline{\mathfrak{c}}}^e$ are obtained analytically. Because of the additive structure of the strain energy, the stress tensor

$$\underline{\boldsymbol{\tau}} = \underline{\boldsymbol{\tau}}_{vol} + \underline{\boldsymbol{\tau}}_{iso} = JU'\underline{\mathbf{1}} + 2\operatorname{dev}\left[\frac{\partial W}{\partial \overline{\underline{\mathbf{b}}}}\overline{\underline{\mathbf{b}}}\right] \tag{71}$$

is splitted into the hydrostatic pressure and the deviatoric component. In order to obtain an iterative solution procedure for the nonlinear system of equations, the resulting formulation is linearized in closed form. Similarly to the computation of the stresses the general form of the elastic tangent operator

$$\underline{\underline{\mathfrak{C}}}^{e} = \underline{\underline{\mathfrak{C}}}^{e}_{vol} + \underline{\underline{\mathfrak{C}}}^{e}_{iso} \tag{72}$$

is composed of a volumetric

$$\underline{\underline{\mathfrak{C}}}^{e}_{vol} = J^2 U''(\underline{\mathbf{1}} \otimes \underline{\mathbf{1}}) + J\, U'(\underline{\mathbf{1}} \otimes \underline{\mathbf{1}} - 2\underline{\underline{\mathbf{I}}}) \tag{73}$$

and an isochoric material tensor

$$\begin{aligned} \underline{\underline{\mathfrak{C}}}^{e}_{iso} = & \frac{2}{3}\,\mathrm{tr}\,\underline{\boldsymbol{\tau}}\left[\underline{\underline{\mathbf{I}}} - \frac{1}{3}\,(\underline{\mathbf{1}} \otimes \underline{\mathbf{1}})\right] - \frac{2}{3}(\mathrm{dev}\,\underline{\boldsymbol{\tau}} \otimes \underline{\mathbf{1}} \\ & + \underline{\mathbf{1}} \otimes \mathrm{dev}\,\underline{\boldsymbol{\tau}}) + 4\,\mathrm{dev}\left[\overline{\underline{\mathbf{b}}}\,\frac{\partial^2 W}{\partial \overline{\underline{\mathbf{b}}}^2}\,\overline{\underline{\mathbf{b}}}\right] \end{aligned} \tag{74}$$

where $\underline{\mathbf{1}}$ and $\underline{\underline{\mathbf{I}}}$ are second order and fourth order unity tensors, respectively. First and second order derivatives of U with respect to J are denoted U' and U''.

References

Aklonis, J. J.; MacKnight, W. J. (1983): Introduction to polymer viscoelasticity. Second Edition. New York: John Wiley

Atluri, S. N.; Reissner, E. (1989): On the formulation of variational theorems involving volume constraints. Computational Mechanics 5: 337–344

Bagley, R. L.; Torvik, P. J. (1983): A theoretical basis for the application of fractional calculus to viscoelasticity. Journal of Rheology 27: 201–210

Baumgaertel, M.; Winter, H. H. (1989): Determination of discrete relaxation and retardation time spectra from dynamic mechanical data. Rheologica Acta 28: 511–519

Bogert, P. A. J. van den; Borst, R. de (1994): On the behaviour of rubberlike materials in compression and shear. Archive of Applied Mechanics 64: 136–146

Christensen, R. M. (1982): Theory of viscoelasticity. Second Edition. London: Academic Press

Eisele, U. (1990): Introduction to polymer physics. Berlin: Springer

Emri, I.; Tschoegl, N. W. (1993): Generating line spectra from experimental responses. Part I: relaxation modulus and creep compliance. Rheologica Acta 32: 311–321

Findley, W. N.; Lai, J. S.; Onaran, K. (1976): Creep and relaxation of nonlinear viscoelastic materials. Amsterdam: North-Holland

Flory, P. J. (1961): Thermodynamic relations for high elastic materials. Transactions of the Faraday Society 57: 829–838

Govindjee, S.; Simo, J. C. (1992): Mullins' effect and the strain amplitude dependence of the storage modulus. International Journal of Solids and Structures 29: 1737–1751

Herrmann, L. R.; Peterson, F. E. (1968): A numerical procedure for viscoelastic stress analysis. In: Proceedings of the Seventh Meeting of ICRPG Mechanical Behavior Working Group. Orlando

Im, S.; Atluri, S. N. (1987): A study of two finite strain plasticity models: an internal time theory using Mandel's director concept, and a general director concept, and a general isotropic/kinematic-hardening theory. International Journal of Plasticity 3: 163–191

Jagusch, J.; Kaliske, M.; Rothert, H.: On vibrations of tires using finite elements. Submitted to: Tire Science and Technology

Lee, E. H. (1969): Elastic-plastic deformation at finite strains. ASME, Journal for Applied Mechanics 36: 1–6

Lubliner, J. (1985): A model of rubber viscoelasticity. Mechanics Research Communications 12: 93–99

Mahnken, R.; Stein, E. (1994): The identification of parameters for visco-plastic models via finite-element methods and gradient methods. Modelling and Simulation in Materials Science and Engineering 2: 597–616.

Miehe, C. (1994): Aspects of the formulation and finite element implementation of large strain isotropic elasticity. International Journal of Numerical Methods in Engineering 37: 1981–2004

Morman, K. N. (1985): Rubber viscoelasticity – a review of current understanding. Dearborn: Ford Motor Company

Mullins, L. (1969): Softening of rubber by deformation. Rubber Chemistry and Technology 42: 339–362

Ogden, R. W. (1982): Elastic deformations of rubberlike solids. Mechanics of solids. In: Hopkins, H. G.; Sewell, M. J. (eds.): The Rodney Hill 60th Anniversary Volume. Oxford: Pergamon Press

Padovan, J. (1987): Computational algorithms for FE formulations involving fractional operators. Computational Mechanics 2: 271–287

Schwarzl, F. R.; Staverman, A. J. (1952): Time-temperature dependence of linear viscoelastic behavior. Journal of Applied Physics 23: 838–843

Sidoroff, F. (1974): Un modèle viscoélastique non linéaire avec configuration intermédiaire. Journal de Mécanique 13: 679–713

Simo, J. C. (1987): On a fully three-dimensional finite-strain viscoelastic damage model: formulation and computational aspects. Computer Methods in Applied Mechanics and Engineering 60: 153–173

Simo, J. C.; Taylor, R. L. (1991): Quasi-incompressible finite elasticity in principal stretches. Continuum basis and numerical algorithms. Computer Methods in Applied Mechanics and Engineering 85: 273–310

Taylor, R. L.; Pister, K. S.; Goudreau, G. L. (1970): Thermomechanical analysis of viscoelastic solids. International Journal for Numerical Methods in Engineering 2: 45–59

Tschoegl, N. W. (1989): The phenomenological theory of linear viscoelastic behavior. Berlin: Springer

Tschoegl, N. W.; Emri, I. (1993): Generating line spectra from experimental responses. Part II: storage and loss functions. Rheologica Acta 32: 311–321

Williams, M. L.; Landel, R. F.; Ferry, J. D. (1955): The temperature dependence of relaxation mechanisms in amorphous polymers and other glass-forming liquids. Journal of the American Chemistry Society 77: 3701–3707